Published OnlineFirst July 24, 2015; DOI: 10.1158/0008-5472.CAN-14-3702

Tumor and Stem Cell Biology

Cancer Research

KAT6B Is a Tumor Suppressor Histone H3 Lysine 23 Acetyltransferase Undergoing Genomic Loss in Small Cell Lung Cancer

Laia Simó-Riudalbas[1], Montserrat Pérez-Salvia[1], Fernando Setien[1], Alberto Villanueva[2], Catia Moutinho[1], Anna Martínez-Cardús[1], Sebastian Moran[1], Maria Berdasco[1], Antonio Gomez[1], Enrique Vidal[1], Marta Soler[1], Holger Heyn[1], Alejandro Vaquero[3], Carolina de la Torre[4], Silvia Barceló-Batllori[4], August Vidal[5], Luca Roz[6], Ugo Pastorino[7], Katalin Szakszon[8], Guntram Borck[9], Conceição S. Moura[10], Fátima Carneiro[11], Ilse Zondervan[12], Suvi Savola[12], Reika Iwakawa[13], Takashi Kohno[13], Jun Yokota[13,14], and Manel Esteller[1,15,16]

Abstract

Recent efforts to sequence human cancer genomes have highlighted that point mutations in genes involved in the epigenetic setting occur in tumor cells. Small cell lung cancer (SCLC) is an aggressive tumor with poor prognosis, where little is known about the genetic events related to its development. Herein, we have identified the presence of homozygous deletions of the candidate histone acetyltransferase *KAT6B*, and the loss of the corresponding transcript, in SCLC cell lines and primary tumors. Furthermore, we show, *in vitro* and *in vivo*, that the depletion of KAT6B expression enhances cancer growth, while its restoration induces tumor suppressor–like features. Most importantly, we demonstrate that KAT6B exerts its tumor-inhibitory role through a newly defined type of histone H3 Lys23 acetyltransferase activity. *Cancer Res; 75(18); 3936–45. ©2015 AACR.*

Introduction

Small cell lung cancer (SCLC) accounts for about 15% of all lung cancers and is characterized by accelerated growth, frequent metastases, and premature death (1). Although SCLC patients demonstrate many times a complete initial response to chemotherapy, the tumor almost always returns probably due to the original presence of quiescent cells. If the total cancer volume is irradiated, survival of SCLC patients is improved. Importantly, we have poor second-line therapies especially when the cancer comes back quickly after first-line therapy is completed. In this regard, no new biologically targeted therapeutics have shown activity in this tumor type (2). Comprehensive genomic analyses have revealed genetically altered therapeutic targets in non–small cell lung carcinoma (3), but little is known about the genetic events involved in SCLC beyond the long-recognized high rate of *TP53* and *RB1* mutations (1). Molecular studies in SCLC have been hampered because these tumors are rarely resected, resulting in a lack of suitable tumor specimens. However, point mutations in genes encoding histone modifiers in SCLC have recently been described (4). In this regard, disruption of the histone modification landscape is a common event in cancer cells (5, 6), leading to significant changes in chromatin structure and gene expression affecting oncogenes and tumor suppressor genes (7, 8). In this context, much effort has been devoted to analyzing the exomes of histone modifiers in search of small nucleotide changes, but cancer-specific copy-number changes have not been particularly studied in profound detail. To address this issue, we have examined the existence of this type of gross genomic alteration for histone modifiers in SCLC that can functionally contribute to the tumoral phenotype and that are of translational relevance.

Materials and Methods

Cell lines and primary tumor samples

Cell lines were purchased from the ATCC (WI-38, NCI-H1963, NCI-H740, NCI-H2171, NCI-H1048, NCI-N417, DMS-114, NCI-

[1]Cancer Epigenetics Group, Cancer Epigenetics and Biology Program (PEBC), Bellvitge Biomedical Research Institute (IDIBELL), Barcelona, Catalonia, Spain. [2]Translational Research Laboratory, Catalan Institute of Oncology (ICO), IDIBELL, Barcelona, Catalonia, Spain. [3]Chromatin Biology Group, IDIBELL, Barcelona, Catalonia, Spain. [4]Proteomics Unit at PEBC, IDIBELL, Barcelona, Catalonia, Spain. [5]Department of Pathology, Bellvitge University Hospital, IDIBELL, Barcelona, Catalonia, Spain. [6]Tumor Genomics Unit, Department of Experimental Oncology and Molecular Medicine, Fondazione IRCCS Istituto Nazionale dei Tumori, Milan, Italy. [7]Thoracic Surgery Unit, Department of Surgery, Fondazione IRCCS Istituto Nazionale dei Tumori, Milan, Italy. [8]Institute of Pediatrics, Clinical Genetics Center, University of Debrecen, Debrecen, Hungary. [9]Institute of Human Genetics, University of Ulm, Ulm, Germany. [10]Department of Pathology, Centro Hospitalar de São João, Porto, Portugal. [11]Institute of Molecular Pathology and Immunology of the University of Porto (IPATIMUP) and Medical Faculty of University of Porto, Porto, Portugal. [12]MRC-Holland, Amsterdam, the Netherlands. [13]Division of Genome Biology, National Cancer Center Research Institute, Tokyo, Japan. [14]Genomics and Epigenomics of Cancer Prediction Program, Institute of Predictive and Personalized Medicine of Cancer (IMPPC), Badalona, Catalonia, Spain. [15]Department of Physiological Sciences II, School of Medicine, University of Barcelona, Barcelona, Catalonia, Spain. [16]Institucio Catalana de Recerca i Estudis Avançats (ICREA), Barcelona, Catalonia, Spain.

Note: Supplementary data for this article are available at Cancer Research Online (http://cancerres.aacrjournals.org/).

Corresponding Author: Manel Esteller, Cancer Epigenetics and Biology Program (PEBC), 3rd Floor, Hospital Duran i Reynals, Av.Gran Via de L'Hospitalet 199–203, 08908 L'Hospitalet de Llobregat, Barcelona, Catalonia, Spain. Phone: 34-93-2607253; Fax: 34-93-2607219; E-mail: mesteller@idibell.cat

doi: 10.1158/0008-5472.CAN-14-3702

Published OnlineFirst July 24, 2015; DOI: 10.1158/0008-5472.CAN-14-3702

H1672, and NCI-H2029), from the Leibniz Institute DSMZ (Jena, Germany)-German Collection of Microorganisms and Cell Cultures (HCC-33), and from Sigma-Aldrich (DMS-273). All cell lines were characterized by short tandem repeat (STR) analysis profiling (LGS Standards SLU) within 6 months after receipt. DNA samples from primary and metastatic tumors of SCLC patients were obtained at surgery or autopsy from 1985 to 2010 at the National Cancer Center Hospital/National Cancer Center Biobank (Tokyo, Japan), Saitama Medical University (Saitama, Japan), and University of Tsukuba (Ibaraki, Japan). The study was approved by the corresponding Institutional Review Boards.

Genotyping microarrays and MLPA analysis

Illumina HumanOmni5-Quad (v1) genotyping array was processed as previously described (9). For multiplex ligation-dependent probe amplification (MLPA), genomic DNA was subjected to SALSA probemixes containing probes for the *KAT6B* gene, in addition to 21 reference probes, and the analyses were performed using Coffalyser.net software (MRC-Holland).

FISH analysis

The UCSC genome browser was used to select the 10q22.2 region probe for *KAT6B* detection (RP11-668A2), and the telomeric probe in 10p15.3 (RP11-361E18) was used as a control. Bacterial artificial chromosome (BAC) clones were obtained from the BACPAC Resource at the Children's Hospital Oakland Research Institute (Oakland, CA). Probes were labeled with Spectrum Green and Red dUTP (Abbott).

Quantitative genomic PCR

The deletion frequency of *KAT6B* (evaluated by SYBR Green) was calculated by the standard curve method using the 7900HT SDS program. Results are reported as the *n*-fold copy number increase relative to the *KAT6B* gene (10q22.3).

Expression and chromatin immunoprecipitation analysis

qRT-PCR, immunoblotting, immunohistochemistry, and chromatin immunoprecipitation (ChIP) assays were performed as previously described (9). For microarray expression array analysis, total RNA from NCI-N417 and HCC-33 cells expressing two different short hairpin RNA (shRNA) sequences against KAT6B and two different scrambled sequences was labeled and hybridized onto a Human Gene Expression G3 v2 60K array following the manufacturer's instructions. qRT-PCR/ChIP primers and antibodies are described in Supplementary Table S1.

KAT6B mutational screening

KAT6B mutations were screened in complementary DNA from 60 SCLC patients and the SCLC lines using direct sequencing (primers in Supplementary Table S1).

Short hairpin interference and ectopic expression assays

Two hairpin RNA (shRNA) molecules targeting two different gene sequences of KAT6B mRNA (shRNA5 and shRNA8) were designed and transfected into NCI-N417 and HCC-33 cells. The described sequences were mutated in two sites to obtain two shRNA scrambled sequences (Supplementary Table S1). For ectopic expression experiments, cDNA from human KAT6B longest isoform was purchased from BioSource (I.M.A.G.E. predicted full-length cDNA clones IRCBp5005P0112Q). *KAT6B* gene was subcloned from pCR-XL-TOPO bacterial expression vector to pRetroX-Tight-Pur mammalian expression vector, within the Retro-XTM Tet-On Advanced Inducible Expression System. A FLAG-tag in the carboxy-terminal end of the protein separated by a flexible Gly–Ser–Gly sequence was introduced.

In vitro proliferation assays

Cell proliferation was determined by the 3-(4,5-dimethyl-2-thiazolyl)-2,5-diphenyl-2H-tetrazolium bromide (MTT) and XTT (2,3-Bis-(2-Methoxy-4-Nitro-5-Sulfophenyl)-2H-Tetrazolium-5-Carboxanilide) assays. The soft agar colony formation assay was performed in 6-well culture plates. Cell proliferation was also determined by counting living cells in the Neubauer chamber using the Trypan blue approach. For dose–response assays, 10,000 to 20,000 cells were seeded in 96-well plates.

Mouse xenograft and metastasis models

Athymic nude male mice were subcutaneously injected in each flank with a total of 3.5×10^6 scramble NCI-N417 cells ($n = 10$) and shRNA NCI-N417 cells ($n = 10$). Tumor growth was monitored every 3 to 4 days by measuring tumor width and length. Pieces (3 mm^3) of subcutaneous mouse tumors were implanted in mouse lungs to generate an orthotopic SCLC mouse model (8 animals for each experiment). For the drug experiments, either irinotecan (24 mg/kg) or vehicle (saline buffer) was injected into the peritoneal cavity once a week for 3 weeks. For the metastasis model, 1.5×10^6 cells were injected into the spleen of 24 mice. Hepatic metastases were examined macroscopically and microscopically. Mouse experiments were approved by the IDIBELL Animal Care Committee.

LC/MS-MS, protein sequence database searching, and SRM

Histone extracts were loaded into an 18% acrylamide/bisacrylamide gel and the histone H3 bands were excised and trypsin-digested. Peptide extracts were analyzed by liquid chromatography-tandem mass spectrometry (LC/MS-MS) using an EASY nLC II (Proxeon) coupled to an amaZon ETD Ion Trap. Data were generated with Data Analyst 4.1 software. MS and MS/MS data were analyzed with ProteinScape 3.1.2 software using Mascot 2.4.0 as the search engine and SwissProt database. Identification was verified using a nanoACQUITY UPLC (Waters) chromatographer coupled to a high-resolution LTQ Orbitrap VelosTM MS. H3K23 acetylation levels were quantified by selected reaction monitoring (SRM) analyzing the precursor and fragment ion masses from acetylated peptides on a hybrid triple quadrupole/ion trap mass spectrometer instrument.

In vitro histone acetylation assays

Histone acetyltransferase assays were performed with GST-Flag–tagged KAT6B HAT domain purified from *Escherichia coli*. One hundred nanograms of HAT domain was incubated in 20 μmol/L [acetyl-1-14C] coenzyme A and 1 μg core histones for 2 hours at 30°C. Incorporated ^{14}C was detected by fluorography with low-energy intensifying screen and loading was assessed by Coomassie staining. For H3K23ac Western blot analysis, histone acetyltransferase assays using core histones as substrate and unlabeled acetyl coenzyme A as cofactor were performed. Recombinant GST-Histone H3 was purified from *E. coli* and used as substrates (1 μg) in the second radioactive histone acetylation assay.

Published OnlineFirst July 24, 2015; DOI: 10.1158/0008-5472.CAN-14-3702

Results

Presence of *KAT6B* homozygous deletion in SCLC that leads to gene inactivation

We first screened a collection of 10 human SCLC cell lines for copy-number alterations in histone-modifier genes using the Illumina Infinium HumanOmni5 microarray, which interrogates 4,301,332 SNPs per sample. These included HCC-33, NCI-N417, NCI-H1048, NCI-H1963, NCI-H2029, DMS-114, DMS-273, NCI-H740, NCI-H2171, and NCI-H1672. Primary normal tissues, such as lung epithelium and leukocytes, were used as normal copy-number control samples. Microarray SNP data have been deposited at the Gene Expression Omnibus (GEO) under accession number GSE62775. Using this approach, we confirmed the presence of previously described aberrant copy number changes in a subset of SCLC cell lines of histone modifiers, such as the CBP histone acetyltransferases (homozygous deletion; ref. 10) and the histone methyltransferase SETDB1 (gene amplification; ref. 9). However, and most interestingly, we found a previously unreported homozygous deletion of the candidate K(lysine) acetyltransferase 6B (*KAT6B*; refs. 11–13), also known as *MYST4* and *MORF*, in two of the 10 (20%) SCLC cell lines: NCI-H1963 (463,888 bp) and NCI-H740 (780,137 bp; Fig. 1A). The tumor suppressor *PTEN*, undergoing also homozygous deletion in SCLC (14) and located 12,830,231 bp far away from the *KAT6B* gene, was not included within the described minimal deleted regions. *KAT6B* undergoes genomic translocation in subtypes of acute myeloid

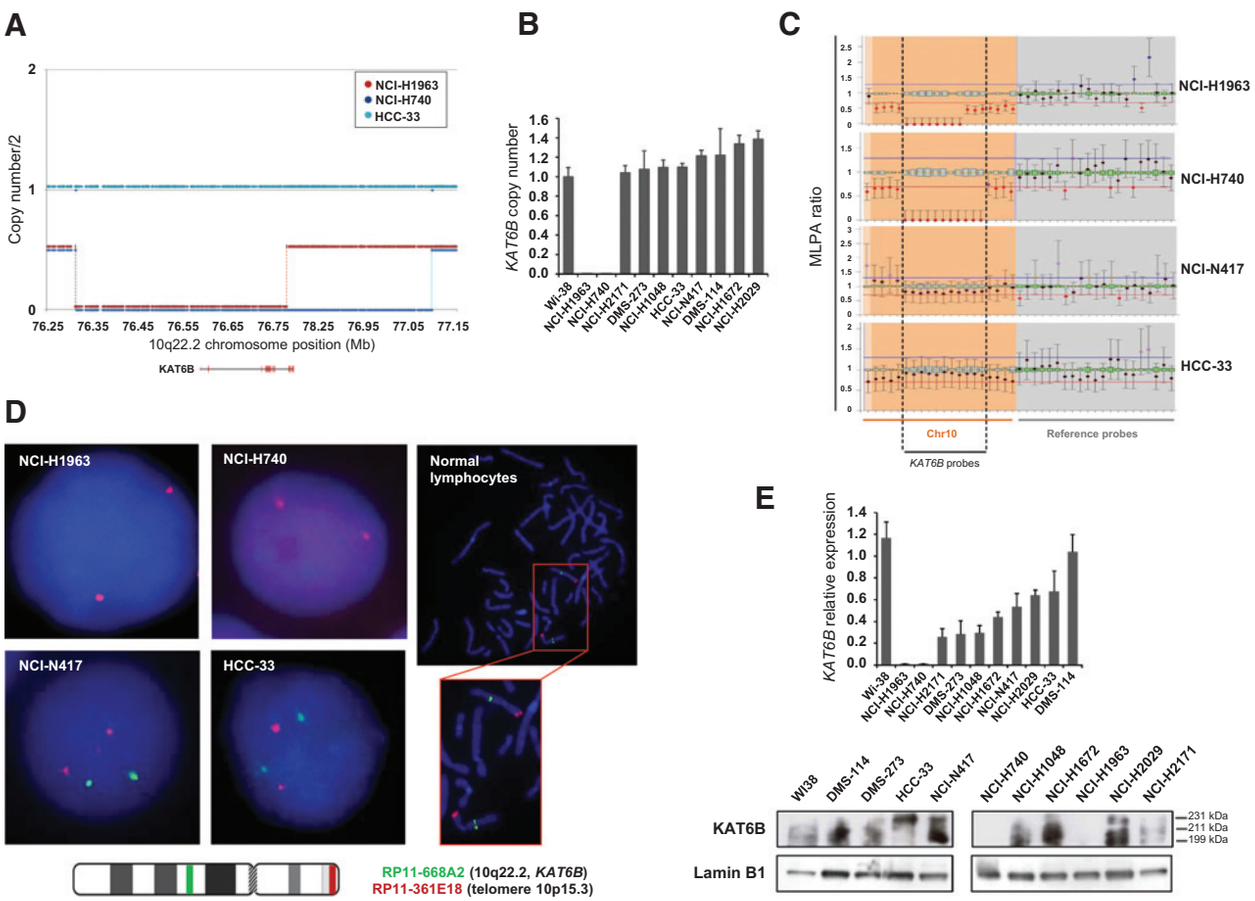

Figure 1.
Determination of *KAT6B* gene homozygous deletion and its association with RNA and protein loss in SCLC cell lines. A, graph depicting the homozygously deleted *KAT6B* region in 10q22.2, identified with the Illumina Infinium HumanOmni5 microarray. The NCI-H1963 cell line has the smallest deleted region (463,888 bp) that encompasses the *KAT6B* gene. NCI-H740 has a homozygously deleted region of (780,137 bp). HCC-33 is shown as an example of an SCLC cell line with two *KAT6B* normal copies. B, assessment of *KAT6B* copy number by quantitative genomic PCR. The amplification frequency of *KAT6B* was calculated by the standard curve method using the 7900HT SDS program. DNA from normal lung fibroblasts (Wi-38) was used as the reference standard. C, MLPA assay. Two different probe mixes contain one probe for each exon of the *KAT6B* gene, two probes upstream and one probe for intron 3 (orange). Twenty reference probes are included (gray). MLPA images from one of the two probe mixes are shown. Values of 0 were considered as homozygous loss. NCI-H1963 and NCI-H740 cell lines show the *KAT6B* homozygous deletion, while HCC-33 and NCI-N417 are shown as examples of *KAT6B* two copy number cells. D, FISH of the *KAT6B* gene. The UCSC Genome Browser was used to select the BAC clone spanning the 10p15.3 region for the *KAT6B* gene, RP11-361E18. A telomeric BAC clone located in the telomeric 10p15.3 region was used as a control. Probes were verified to give a single signal on normal commercial lymphocyte metaphase slides. E, quantitative reverse transcription PCR (top) and Western blot analysis (bottom) demonstrate loss of KAT6B mRNA and protein (the three existing isoforms are shown), respectively, in homozygously deleted NCI-H1963 and NCI-H740 cells.

leukemia (15, 16) and uterine leiomyomata (17), and *KAT6B* mutations have also been recently associated with the development of genitopatellar syndrome and Say-Barber-Biesecker-Young-Simpson syndrome (SBBYSS or Ohdo syndrome; refs. 18–20). Data mining of the Cancer Cell Line Encyclopedia copy-number variation data derived from a lower resolution SNP microarray (21) confirmed the presence of the *KAT6B* homozygous deletion in NCI-H1963 (Supplementary Fig. S1), while NCI-H740 was not included in the described study. Using a quantitative genomic PCR approach (Fig. 1B), MLPA (Fig. 1C) and fluorescence *in situ* hybridization (FISH; Fig. 1D), we confirmed the presence of the *KAT6B* homozygous deletion in NCI-H1963 and NCI-H740. The remaining eight SCLC cell lines did not exhibit any homozygous loss of *KAT6B* (Fig. 1A–D). *KAT6B* 5′-CpG island promoter methylation was not found in any SCLC cell line (Supplementary Fig. S1). Copy number and RNA expression levels for other histone acetyltransferases in the studied SCLC cell lines are shown in Supplementary Fig. S2. The SCLC cell lines underwent mutational screening for the 18 exons of the *KAT6B* gene using direct Sanger sequencing. The only nucleotide change that we detected was, in the NCI-H1048 cell line, a deletion of a GAA triplet coding for a glutamic acid within a stretch of glutamic amino acids in exon 16: it has been described as a polymorphic variant in the COSMIC Sanger database. Splicing defects were not specifically sought and could be another mechanism of gene silencing. Using quantitative reverse-transcription PCR and Western blot analysis, we found that the expression of KAT6B for both mRNA and protein was lost in the SCLC cancer cell lines NCI-H1963 and NCI-H740, which harbor the *KAT6B* homozygous deletion (Fig. 1E and Supplementary Fig. S3).

KAT6B has tumor suppressor–like properties in cancer cells

Once we had demonstrated the presence of *KAT6B* genomic loss in the SCLC cell lines, we examined its contribution to the tumorigenic phenotype *in vitro* and *in vivo*. We first analyzed the effect of KAT6B depletion in lung cancer cells retaining both copies of genes such as HCC33 and N417 (Fig. 2A and Supplementary Fig. S3). Supplementary Table S1 illustrates the shRNA sequences used. We observed that the reduction of KAT6B expression in the described cells, compared with the scramble shRNAs, had cancer growth-enhancing features, such as increased viability in the MTT assay (Fig. 2B), and formed more colonies (Fig. 2C). The XTT assay and Trypan blue staining further confirmed the growth-enhancing features of KAT6B-induced depletion (Supplementary Fig. S4). Interestingly, we observed that KAT6B shRNA-depleted cells also showed diminished expression of Brahma (BRM), a known KAT6B target (Supplementary Fig. S4; ref. 22), and the BRM-target E-cadherin (Supplementary Fig. S4; ref. 23), both being proteins that influence cell proliferation and metastasis. shRNA-mediated depletion of KAT6B also induced an increase in Rb phosphorylation (Supplementary Fig. S4). We next tested the ability of KAT6B shRNA-transfected N417 cells to form subcutaneous tumors in nude mice compared with scramble shRNA-transfected cells (Fig. 2D). Cells with shRNA-mediated depletion of KAT6B formed tumors with a greater weight and volume, but N417-scramble shRNA-transfected cells showed much lower tumorigenicity (Fig. 2D). We then performed an orthotopic growth study, implanting equal-sized tumor pieces from the subcutaneous model in the lung. We observed that orthotopic KAT6B shRNA-depleted tumors were significantly bigger and heavier than the scramble shRNA-derived tumors (Fig. 2E). We also proceeded with the converse experiment in which we used a retroviral-inducible expression system to recover by transfection the expression of KAT6B (longest isoform, 231 kDa) in H1963 cells bearing the aforementioned homozygous gene deletion (Fig. 2F). H1963 cells transfected with either the empty or the KAT6B vector were subcutaneously injected into the nude mice. Tumors originated from KAT6B-transfected H1963 cells had a significantly smaller volume than empty vector–transfected-derived tumors after doxycycline activation of gene expression (Fig. 2F). The halt in cellular growth upon restoration of KAT6B expression was observed for a long period of time (49 days; Supplementary Fig. S4). Finally, the potential distant inhibitory dissemination activity of KAT6B was measured in athymic mice by direct spleen injection and analysis of metastasis formation in the liver (Fig. 2G). Whereas numerous metastatic nodules developed in the liver following injection of KAT6B shRNA-depleted empty N417 cells, less metastasis formation was observed with the scramble shRNA-transfected cells (Fig. 2G). Overall, our findings suggest tumor-suppressor and dissemination-inhibitor roles for KAT6B.

Lysine 23 of histone H3 as a target of KAT6B-mediated acetylation

We next wondered about the molecular mechanisms that could mediate the identified tumor-suppressor features of KAT6B. In trying to address this issue, we first encountered the serious obstacle that the histone lysine residues targeted for acetylation by human KAT6B have not been completely characterized *in vivo*. KAT6B is a member of the MYST family of histone acetyltransferases that also includes KAT6A (MYST3/MOZ), KAT7 (MYST2/HBO1), KAT5 (Tip60), and KAT8 (MYST1/MOF; Fig. 3A). Because of the greater homology of KAT6B with the *bona fide* histone H3 acetyltransferase KAT6A (24–26), which also undergoes genomic translocations in acute myelogenous leukemia (27, 28), and the initially reported *in vitro* specificity of the KAT6A/KAT6B complex for histone H3 but not for histone H4 (29, 30), we focused our interest on this particular histone. To identify the histone H3 target sites for KAT6B, we compared H1963 cells transduced with an empty vector or with the full-length KAT6B expression vector (Fig. 3B). We used histone acid extracts resolved in an SDS–PAGE gel, followed by digestion of the histone H3 band and LC/MS-MS analysis. We determined from precursor signal intensity of the two acetylated peptides, K.QLATK^{23ac}AAR and R.KQLATK^{23ac}AAR.K, that acetylation of H3-K23 was enriched upon KAT6B transfection in H1963 cells (Fig. 3C). Targeted quantification of acetylation of H3-K23 residue by SRM confirmed the enhancement of this acetylated residue upon transduction-mediated recovery of KAT6B expression in the H1963 cell line (Fig. 3D). Using SRM, we were also able to study a patient with the SBBYS type of Ohdo syndrome, who was carrying truncating mutation of KAT6B (31, 32), and who showed a reduced level of both acetylated H3-K23 peptides (Fig. 3D). Western blot analyses also confirmed the LC/MS-MS data by showing that H3-K23 acetylation increased upon KAT6B transfection in H1963 cells (Fig. 3E). The activity of KAT6B for acetyl-K23 H3 was confirmed by Western blot analysis in two additional models: KAT6B shRNA-depleted N417 cells showed a reduction of the described acetylation

Published OnlineFirst July 24, 2015; DOI: 10.1158/0008-5472.CAN-14-3702

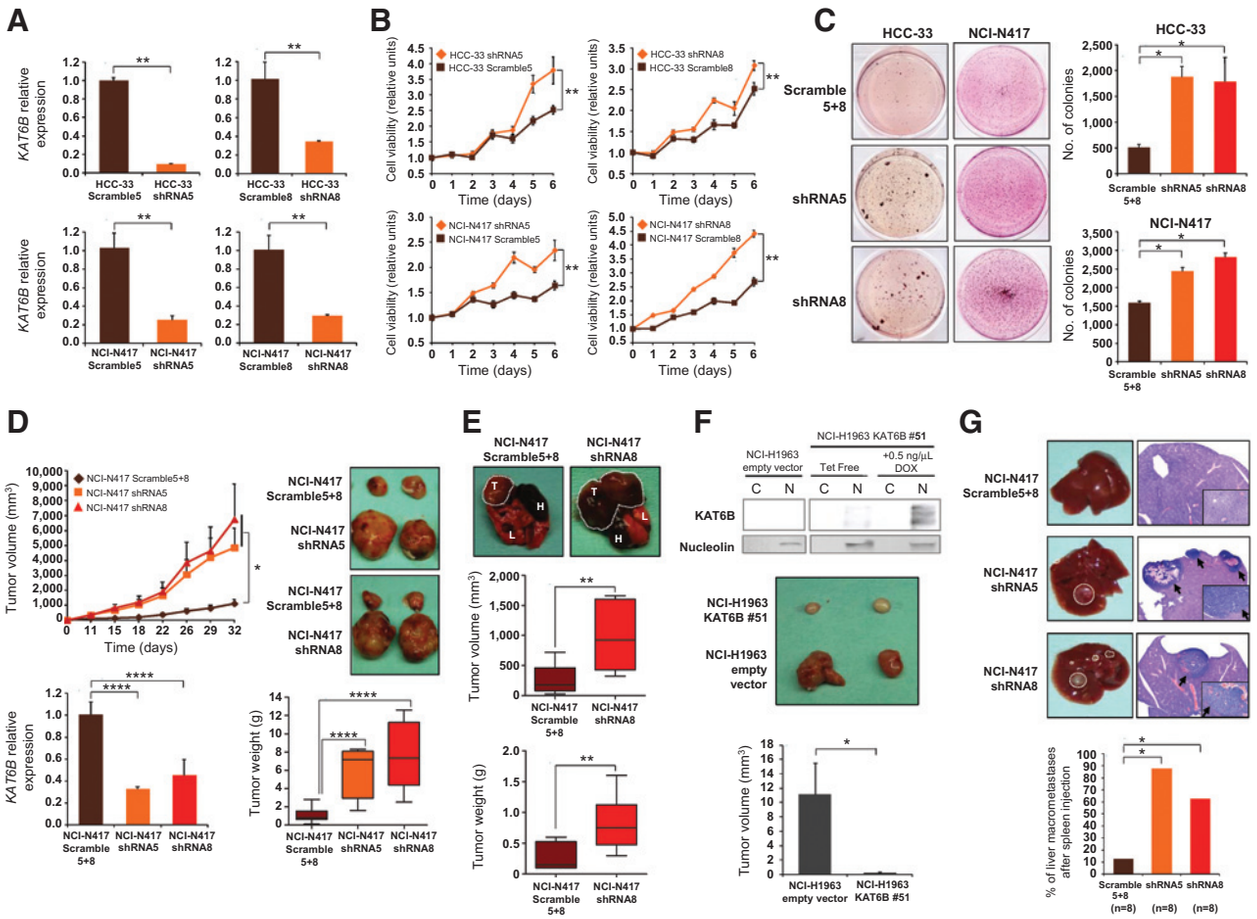

Figure 2.

Growth-inhibitory effects of KAT6B in SCLC. A, downregulation of the *KAT6B* gene by short hairpins using two target sequences (shRNA5 and shRNA8) in NCI-N417 and HCC-33 cells. Significance of permutation tests, **, $P < 0.01$. B, the short hairpin KAT6B-depleted cells were significantly more viable in the MTT assay than in the scrambled shRNA-transfected cells. Significance of ANOVAs, **, $P < 0.01$. C, the colony formation assay showed that NCI-N417 and HCC-33 cells transfected with the shRNA against KAT6B formed significantly more colonies than did scrambled shRNA-transfected cells. Data are mean ± SEM ($n = 3$). Significance of permutation tests, *, $P < 0.05$. D, effect of KAT6B shRNA-mediated depletion on the growth of subcutaneous tumors in nude mice derived from NCI-N417 cells. There was a significant increase in tumor volume and weight in the KAT6B shRNA-depleted cells. Data are mean ± SEM ($n = 10$). Low KAT6B mRNA levels in shRNA5 and shRNA8 NCI-N417 tumors confirmed the stability of the transfection after 32 days. ANOVAs, *, $P < 0.05$; ****, $P < 0.0001$. E, KAT6B shRNA-mediated depletion also significantly increased the volume and weight of orthotopic tumors derived from NCI-N417 cells implanted in the lung of nude mice. Significance of permutation tests, *, $P < 0.05$. F, recovery of KAT6B expression in NCI-H1963 cells (top), using a retroviral transfection Tet-ON system, decreased the volume of subcutaneous tumors implanted in nude mice (bottom). Significance of permutation test, *, $P < 0.05$. G, KAT6B shRNA-depleted NCI-N417 cells show significantly higher dissemination capacity after spleen injection. Illustrative surgery samples and hematoxylin and eosin staining of colonized liver after spleen injection are shown. Fisher exact test, *, $P < 0.05$.

mark (Fig. 3E), and the aforementioned SBBYS type of Ohdo syndrome patient with the *KAT6B* truncating mutation also had a lower level of acetylated H3-K23 (Fig. 3E). KAT6B specificity for this histone residue was further demonstrated by showing that acetylation of lysine 14 of histone H3 and lysine 16 of histone H4, mediated by the MYST family members KAT6A (MYST3/MOZ; refs. 25, 26, 29) and KAT8 (MYST1/MOF; refs. 33, 34), respectively, were not modified upon KAT6B restoration, depletion, or mutation (Fig. 3E). We also developed *in vitro* histone acetylation assays to further show the activity of KAT6B for H3K23 acetylation. Using purified histone core proteins from HeLa cells and a construct for the KAT6B-specific HAT domain, we confirmed that it acetylated H3-K23 (Supplementary Fig. S5). Importantly, a mutant HAT domain protein for KAT6B in K815, a strictly conserved lysine residue in the MYST family (35), was unable to acetylate H3-K23 (Supplementary Fig. S5). In addition, the *in vitro* activity of KAT6B for H3-K23 was confirmed using a recombinant histone H3 as a substrate: the wild-type cloned KAT6B-HAT domain acetylated the described residue and the K815 mutant was unable to do so (Supplementary Fig. S5). Using shRNA-mediated depletion of four histone deacetylases (HDAC1, HDAC2, HDCA3, and HDAC6) in NCI-N417 cells, we observed that, upon HDAC1 downregulation, there was an increase in acetylated H3-K23 levels (Supplementary Fig. S5), suggesting that this last HDAC mediates the deacetylation event at this residue.

We next wondered about gene targets whose normal expression could be diminished in cancer cells by the loss of KAT6B-

Published OnlineFirst July 24, 2015; DOI: 10.1158/0008-5472.CAN-14-3702

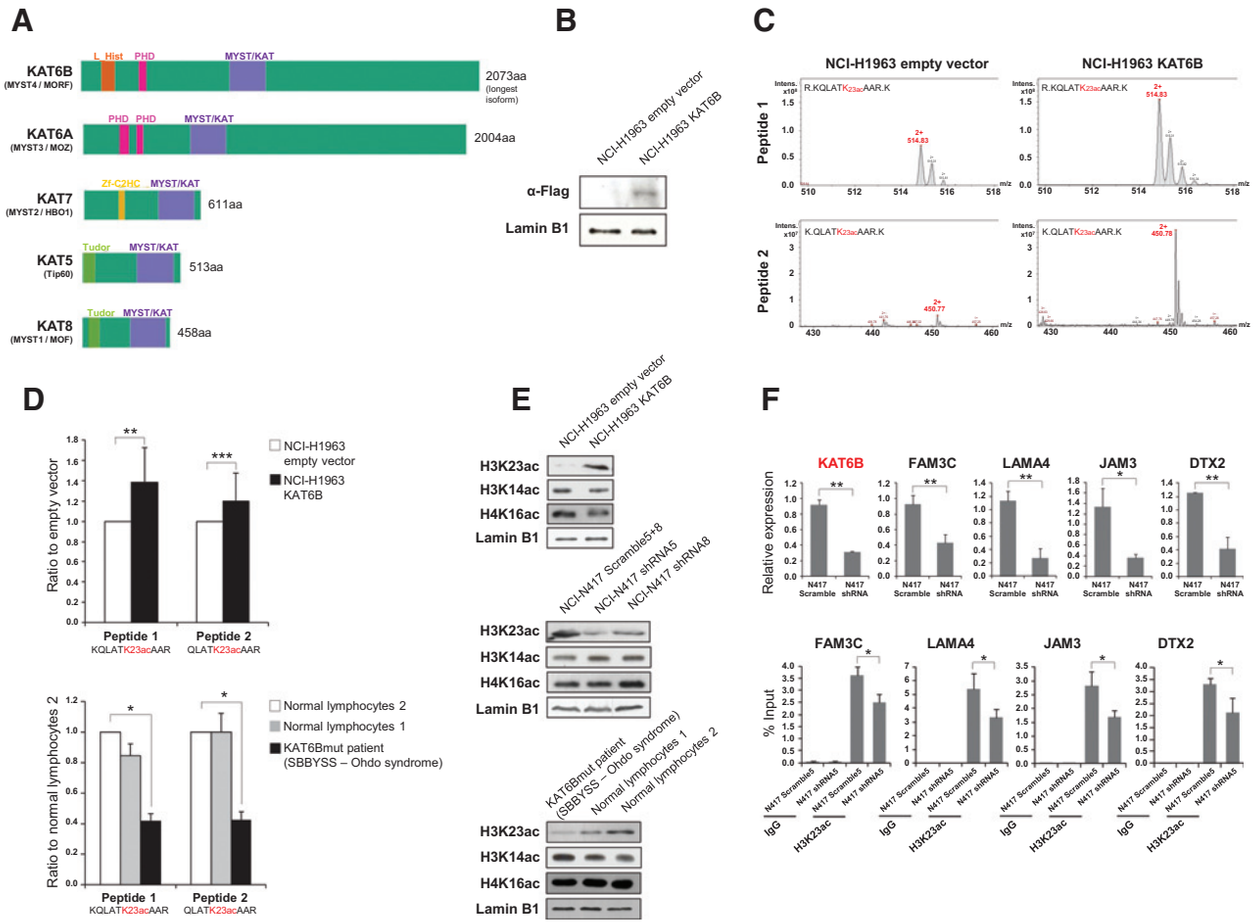

Figure 3.

KAT6B is a histone acetyltransferase targeting lysine 23 of histone H3. A, diagram of the MYST (SAS/MOZ) family with its recognized domains. The domains depicted are: L_Hist, linker histone H1/H5 domain H15; PHD, zinc_finger PHD type; Tudor_knot, RNA binding activity-knot of a chromodomain; Zf-C2HC, zinc finger, C2H2 type; MYST/KAT, MYST-type HAT (histone acetyltransferase) domain. B, Western blot analysis shows efficient transduction of KAT6B in NCI-H1963 cells in comparison with empty vector–transfected cells. C, MS spectra of QLATKacAAR and KQLATKacAAR tryptic peptides identified by LC/MS-MS. A representative figure is shown of the precursor intensity based on the integration of the signal from the extracted ion chromatogram. KAT6B NCI-H1963-transfected cells show a sharp increase in H3K23 acetylation intensity in both of the identified peptides compared with the empty vector–transfected cells. D, SRM quantification of the two H3K23ac peptides. Results were normalized with respect to the transitions of the corresponding heavy synthetic peptide and were related to the empty vector (top) or normal lymphocytes (bottom). Targeted quantification confirms the enhancement of this acetylated residue for the two peptides upon transfection-mediated recovery of KAT6B expression in H1963 cells (top) and its reduction in a patient of SBBYS type of Ohdo syndrome carrying a truncating mutation of *KAT6B* (bottom). Differences between the transitions were examined with the Student *t* test. *, $P < 0.05$; **, $P < 0.01$; ***, $P < 0.001$. E, Western blot analysis confirms the activity of KAT6B for H3K23ac upon transfection in NCI-H1963–deleted cells (top), in KAT6B shRNA-depleted NCI-N417 cells (middle), and in the SBBYSS or Ohdo syndrome patient with the *KAT6B*-truncating mutation (bottom). H3K14ac and H4K16ac did not change in any condition. F, qRT-PCR and H3K23ac ChIP analysis shows that, upon KAT6B-shRNA depletion in NCI-N417 cells, the downregulation of the candidate genes is associated with diminished acetylation of H3K23 residue in the promoters. Permutation tests, **, $P < 0.05$; *, $P < 0.01$.

mediated H3-K23 promoter acetylation, a histone mark usually associated with gene activation. To identify KAT6B target genes that might fit this candidate criterion, we used the shRNA approach to deplete KAT6B expression in N417 and HCC33 (both with the normal two copies of the *KAT6B* gene) followed by expression microarray hybridization. The complete list of genes undergoing expression changes is shown in Supplementary Table S2. Microarray expression data are available at GEO under accession number GSE62775. Using this approach, we identified 32 common genes repressed in both KAT6B-shRNA–depleted lung cancer cell lines that were upregulated in scramble shRNA-transfected cells (Supplementary Table S2). We confirmed the expression changes of 25 candidate genes (78%) by quantitative reverse-transcription PCR (Fig. 3F and Supplementary Fig. S5). The shift in H3-K23 acetylation status in their respective promoters for four candidate genes was observed by quantitative ChIP (Fig. 3F).

KAT6B genomic loss occurs in SCLC patients and confers sensitivity to irinotecan

Finally, we sought to demonstrate that the presence of *KAT6B* homozygous deletion was not a specific feature of *in vitro*–grown SCLC cell lines and that it also occurred in primary tumors of SCLC patients. Herein, we performed MLPA analyses for the

Published OnlineFirst July 24, 2015; DOI: 10.1158/0008-5472.CAN-14-3702

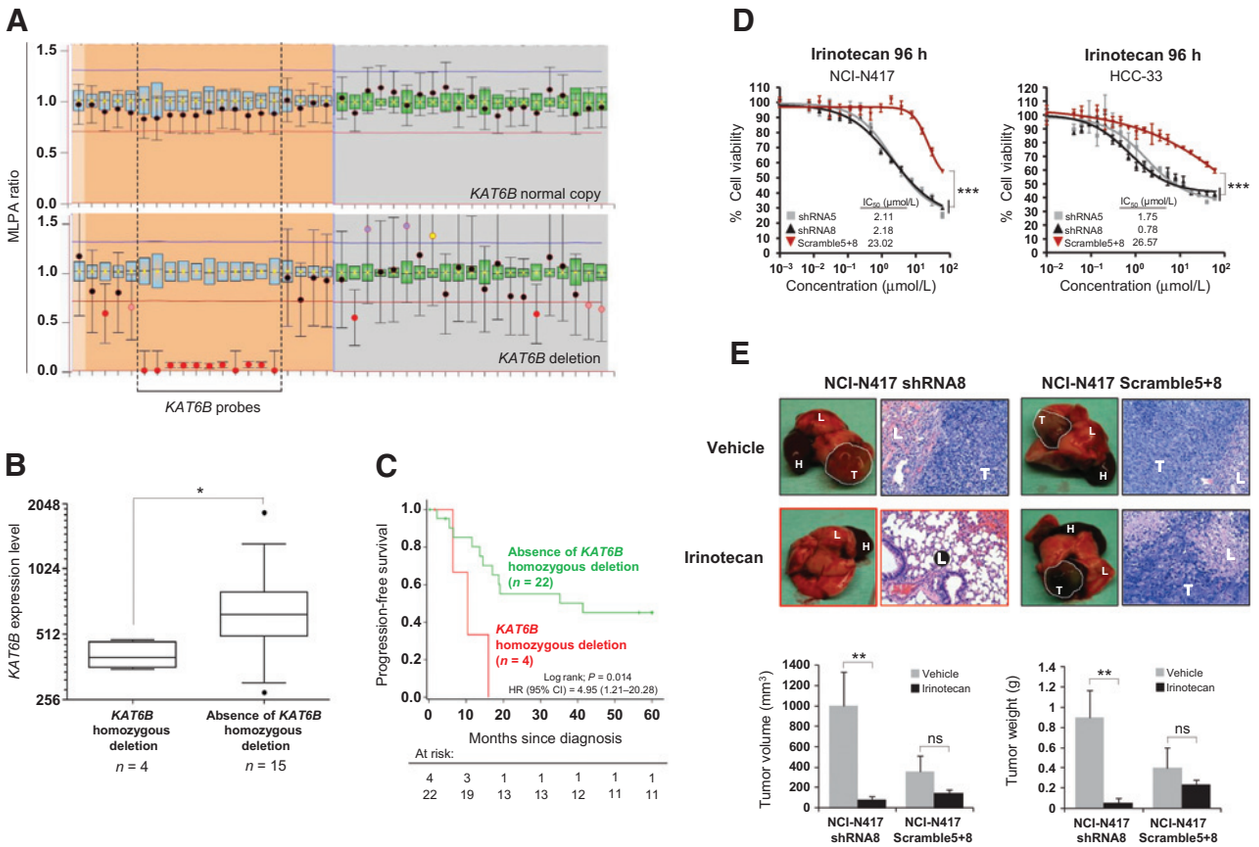

Figure 4.
Genomic loss of *KAT6B* in SCLC patients and sensitivity to irinotecan. A, examples of assessment of *KAT6B* copy number by MLPA in an SCLC patient without loss (top) and in one with homozygous deletion (bottom). B, the presence of *KAT6B* homozygous deletion is significantly associated with loss of expression of the KAT6B transcript in tumors from SCLC patients. The box plots illustrate the distribution of microarray expression values; the central solid line indicates the median; the limits of the box show the upper and lower quartiles. Mann–Whitney test, *, $P < 0.05$. C, the Kaplan–Meier analysis of progression-free survival among a cohort of SCLC cases according to KAT6B genomic status. KAT6B homozygous deletion is significantly associated with a shorter progression-free survival (log-rank test; $P = 0.014$; hazard ratio, 4.95; 95% confidence interval, 1.21–20.28). D, KAT6B shRNA-depleted NCI-N417 and HCC-33 cells were significantly more sensitive to the antiproliferative effect of irinotecan than were shRNA scramble-transfected cells. ANOVAs, ***, $P < 0.001$. E, orthotopic tumors-derived from KAT6B shRNA-depleted NCI-N417 cells were more sensitive to irinotecan than were shRNA scramble-derived tumors according to tumor volume and weight. L, Lung; H, Heart; T, Tumor. Significance of permutation tests, **, $P < 0.01$.

KAT6B locus using a collection of 60 tumors from SCLC patients and identified the *KAT6B* homozygous deletion in eight SCLC tumors (13%; Fig. 4A). Codeletion of *PTEN* was not observed in the SCLC tumors with *KAT6B* genomic loss according to CNV microarray data (36). Interestingly, screening for nonsense and indels in the *KAT6B* coding sequence in these 60 SLC cases, we identified a deletion of a "C" in the last exon (exon 18; c.3824delC) that later creates a stop codon and renders a 798 amino acids shorter protein, suggesting alternative pathways for the inactivation of the studied gene. Microarray expression data were available for 19 of the SCLC patients studied (36), including four who had the *KAT6B* homozygous deletion, and we observed an association between KAT6B genomic loss and lower levels of the transcript (Fig. 4B). Immunohistochemical analyses of 20 SCLC cases showed overall loss of *KAT6B* expression and acetyl-K23 H3 in the four tumors with *KAT6B* deletion, whereas both protein and histone mark were clearly stained in the remaining 16 samples without *KAT6B* genomic loss (except in one case where other mechanisms might account for an observed lack of staining). Illustrative cases are shown in Supplementary Fig. S6. Interestingly, in those SCLC patients for whom we have clinical information and a long follow-up over different stages ($n = 26$), the presence of the *KAT6B* homozygous deletion was associated with significantly shorter progression-free survival (log-rank test; $P = 0.014$; hazard ratio; 4.95; 95% confidence interval, 1.21–20.28; Fig. 4C).

The observation that the *KAT6B* homozygous deletion also occurred in SCLC patients with even worse prognosis prompted us to examine whether the loss of this HAT was associated with a particular sensitivity to any anticancer drug. Similar scenarios have been described for inhibitors of histone methyltransferases, such as DOT1L (37) and the BET family of acetyllysine–recognizing chromatin "adaptor" proteins (38–40) in which hematologic malignancies associated with gene-activating events involving targets of these pathways are more sensitive to these drugs. Using the model of KAT6B shRNA-transfected versus scramble shRNA-transfected N417 cells and the calculation of IC_{50} values according to the MTT assay, we did

Published OnlineFirst July 24, 2015; DOI: 10.1158/0008-5472.CAN-14-3702

not observe any difference between the two types of cells for 28 HDAC inhibitors that target class I, IIA, IIB, and III, in addition to pan-inhibitors (Supplementary Fig. S7). The compounds and their HDAC targets can be found in Supplementary Table S3. In addition, we did not observe any difference in sensitivity for classic SCLC chemotherapy agents such as cisplatin or etoposide (Supplementary Fig. S7). However, we found that KAT6B-depleted cells were significantly more sensitive to the growth-inhibitory effect mediated by the chemotherapy agent irinotecan, under clinical trials in SCLC, than any of the scramble shRNA clones (Fig. 4D). The same result was observed for HCC-33 cells (Fig. 4D). We also extended the *in vitro* cell viability experiments to the *in vivo* mouse model, thereby confirming that orthotopic SCLC tumors derived from KAT6B shRNA-depleted N417 cells were significantly more responsive to irinotecan than scramble shRNA-derived tumors (Fig. 4E). Within our SCLC clinical cohort, 42% of cases (11 of 26) underwent chemotherapy, but mainly platin-based combinations. Only 4 patients received irinotecan-based chemotherapy and none of them had *KAT6B* homozygous deletion. Thus, it was unfeasible to assess the role of *KAT6B* deletion as a predictive factor of irinotecan-based treatment outcome in this setting. Related to why irinotecan could be particularly effective in *KAT6B*-deleted tumors, it has been reported that the MYST family of HATs facilitates ataxia–telangiectasia mutated (ATM) kinase-mediated DNA-damage response (41) and, thus, it is possible that irinotecan-induced DNA damage cannot be so efficiently repaired in the KAT6B deficient tumors, leading to the enhanced cell death. In this regard, we found that KAT6B shRNA-mediated depletion caused a reduction of ATM expression and, upon irinotecan treatment, a lower phosphorylation of H2AX (Supplementary Fig. S8). Overall, these data suggest the existence of a therapeutic "niche" for the use of irinotecan in the aforementioned subset of SCLC cases harboring the *KAT6B* homozygous deletion.

Discussion

The initial high response rates to platinum-based chemotherapy regimens for SCLC in the late 1970s and early 1980s caused great expectations for these therapies. However, these hopes were shattered by the recognition of low 5-year survival rates, in most instances only approximately 5% (1, 2, 42). More recent trials with targeted therapies in SCLC have failed with no new drugs progressing treatments beyond those of cisplatin and etoposide (1, 2, 42). One of the main reasons for this disappointing scenario is our limited knowledge of the molecular driver events in SCLC. Beyond the high prevalence of *TP53* and *RB1* mutations, which have not proven amenable to pharmacology-based therapies so far, we have a scarce knowledge of the genetic defects underlying the natural history of SCLC. A recent breakthrough in this area has been the identification of mutations in histone modifiers, such as the histone methyltransferase *MLL1* or the histone acetyltransferases *CREBBP* (*KAT3A*) and *EP300* (*KAT3B*), in a subset of SCLCs (4). In this context, our identification of *KAT6B* homozygous deletions in both SCLC cell lines and primary tumors upgrades the genetic disruption of histone modifier genes as the second most common class of altered genes in SCLC. Importantly, we define for the first time, an *in vivo* target site for the acetyltransferase activity of KAT6B, lysine 23 of histone H3. This histone posttranslational modification has been previously associated with a more open chromatin state and the transcriptional activation of the underlying DNA sequence (43, 44). Interestingly, the diminished acetylation of H3-K23 seems to be a hallmark of SCLC tumorigenesis, because the other two frequently mutated histone acetyltransferases (CREBBP and EP300) can also target this particular histone amino acid (43–45).

An interesting issue derived from our studies is the potential exploitation of the KAT6B histone acetyltransferase defect to design more personalized therapies that could improve the dismal outcome of SCLC. Epigenetic drugs are the focus of a growing interest in the cancer arena; however, a critical issue is going to be the selection of those patients that are more likely to respond to these compounds. For example, pediatric brainstem gliomas harboring a mutation in K27 of histone H3.3 are more sensitive to the pharmacologic inhibition of a K27 demethylase (46). Herein, we did not observe that KAT6B depletion increases sensitivity to HDAC inhibitors, but other epigenetic inhibitors can be tested in this model. These include bromodomain inhibitors, targeting BET (bromodomain and extra-terminal domain) proteins that "read" the acetylated histone residues (39–41), or inhibitors of histone methyltransferases/demethylases, taking in account the competition between acetylation and methylation that occurs at K23-H3 (47). In addition, because KAT6B tumor-suppressor properties are, in part, mediated by downstream genes, like *BRM*, then might the restoration of these gene(s) be therapeutic. However, we have already found a drug where the diminished expression of KAT6B increases SCLC sensitivity in cell and animal models: irinotecan. Currently, this compound is a second-line treatment for the extensive stage of SCLC, while a platinum agent and etoposide are first-line therapies (1, 2, 42). Interestingly, as irinotecan is an effective drug for other tumor types, such as colon cancer, it would be interesting to explore if KAT6B status is associated with sensitivity to this drug beyond SCLC. Herein, our results pinpoint a subgroup of SCLC patients, those carrying the *KAT6B* genomic loss, where prospective clinical trials to assess the efficacy of irinotecan can be further studied.

Disclosure of Potential Conflicts of Interest

No potential conflicts of interest were disclosed.

Authors' Contributions

Conception and design: A. Villanueva, U. Pastorino, I. Zondervan, M. Esteller
Development of methodology: L. Simó-Riudalbas, M. Pérez-Salvia, F. Setien, A. Villanueva, M. Berdasco, A. Vaquero, C. de la Torre, S. Barceló-Batllori, U. Pastorino, S. Savola
Acquisition of data (provided animals, acquired and managed patients, provided facilities, etc.): A. Villanueva, A. Martínez-Cardús, H. Heyn, A. Vaquero, C. de la Torre, S. Barceló-Batllori, A. Vidal, L. Roz, U. Pastorino, K. Szakszon, G. Borck, I. Zondervan, R. Iwakawa, T. Kohno, J. Yokota, M. Esteller
Analysis and interpretation of data (e.g., statistical analysis, biostatistics, computational analysis): L. Simó-Riudalbas, C. Moutinho, A. Martínez-Cardús, S. Moran, M. Berdasco, A. Gomez, E. Vidal, H. Heyn, A. Vaquero, S. Barceló-Batllori, A. Vidal, C.S. Moura, F. Carneiro, I. Zondervan, S. Savola, M. Esteller
Writing, review, and/or revision of the manuscript: L. Simó-Riudalbas, S. Moran, A. Vidal, L. Roz, G. Borck, C.S. Moura, F. Carneiro, S. Savola, R. Iwakawa, M. Esteller
Administrative, technical, or material support (i.e., reporting or organizing data, constructing databases): C. Moutinho, A. Martínez-Cardús, M. Soler, C. de la Torre, R. Iwakawa, M. Esteller
Study supervision: U. Pastorino, J. Yokota, M. Esteller

Acknowledgments

The authors thank Drs. Masayuki Noguchi, Ryo Nishikawa, Shun-ichi Watanabe, Yoshitaka Narita, and Koji Tsuta for providing SCLC tissues and patients' information.

Grant Support

Supported by the grants FP7/2007-2013 HEALTH-F2-2010-258677–CURELUNG, European Research Council Advanced grants 268626–EPINORC, SAF2011-22803, PIE13/00022-ONCOPROFILE, 13FIS037 and PT13/0001/0033, a Grant-in-Aid from the Ministry of Education, Culture, Sports, Science, and Technology of Japan, a National Cancer Center Research and Development Fund (26-A-1) Cellex Foundation and Catalan Government (2009SGR1315 and 2014SGR633, AGAUR).

The costs of publication of this article were defrayed in part by the payment of page charges. This article must therefore be hereby marked *advertisement* in accordance with 18 U.S.C. Section 1734 solely to indicate this fact.

Received December 22, 2014; revised July 3, 2015; accepted July 19, 2015; published OnlineFirst July 24, 2015.

References

1. van Meerbeeck JP, Fennell DA, De Ruysscher DK. Small-cell lung cancer. Lancet 2011;378:1741–55.
2. Pillai RN, Owonikoko TK. Small cell lung cancer: therapies and targets. Semin Oncol 2014;41:133–42.
3. Buettner R, Wolfm J, Thomas RK. Lessons learned from lung cancer genomics: the emerging concept of individualized diagnostics and treatment. J Clin Oncol 2013;31:1858–65.
4. Peifer M, Fernández-Cuesta L, Sos ML, George J, Seidel D, Kasper LH, et al. Integrative genome analyses identify key somatic driver mutations of small-cell lung cancer. Nat Genet 2012;44:1104–10.
5. Fraga MF, Ballestar E, Villar-Garea A, Boix-Chornet M, Espada J, Schotta G, et al. Loss of acetylation at Lys16 and trimethylation at Lys20 of histone H4 is a common hallmark of human cancer. Nat Genet 2005;37:391–400.
6. Seligson DB, Horvath S, Shi T, Yu H, Tze S, Grunstein M, et al. Global histone modification patterns predict risk of prostate cancer recurrence. Nature 2005;435:1262–6.
7. Berdasco M, Esteller M. Aberrant epigenetic landscape in cancer: how cellular identity goes awry. Dev Cell 2010;19:698–711.
8. Dawson MA, Kouzarides T. Cancer epigenetics: from mechanism to therapy. Cell 2012;150:12–27.
9. Rodriguez-Paredes M, Martinez de Paz A, Simó-Riudalbas L, Sayols S, Moutinho C, Moran S, et al. Gene amplification of the histone methyltransferase SETDB1 contributes to human lung tumorigenesis. Oncogene 2014;33:2807–13.
10. Kishimoto M, Kohno T, Okudela K, Otsuka A, Sasaki H, Tanabe C, et al. Mutations and deletions of the CBP gene in human lung cancer. Clin Cancer Res 2005;11:512–9.
11. Champagne N, Bertos NR, Pelletier N, Wang AH, Vezmar M, Yang Y, et al. Identification of a human histone acetyltransferase related to monocytic leukemia zinc finger protein. J Biol Chem 1999;274:28528–36.
12. Yang XJ, Ullah M. MOZ and MORF, two large MYSTic HATs in normal and cancer stem cells. Oncogene 2007;26:5408–19.
13. Klein BJ, Lalonde ME, Côté J, Yangm X J, Kutateladze TG. Crosstalk between epigenetic readers regulates the MOZ/MORF HAT complexes. Epigenetics 2014;9:186–93.
14. Forgacs E, Biesterveld EJ, Sekido Y, Fong K, Muneer S, Wistuba II, et al. Mutational analysis of the PTEN/MMAC1 gene in lung cancer. Oncogene 1998;17:1557–65.
15. Panagopoulos I, Fioretos T, Isaksson M, Samuelsson U, Billström R, Strömbeck B, et al. Fusion of the MORF and CBP genes in acute myeloid leukemia with the t(10;16)(q22;p13). Hum Mol Genet 2001;10:395–404.
16. Vizmanos JL, Larráyoz MJ, Lahortiga I, Floristán F, Alvarez C, Odero MD, et al. t(10;16)(q22;p13) and MORF-CREBBP fusion is a recurrent event in acute myeloid leukemia. Genes Chromosomes Cancer 2003;36:402–5.
17. Moore SD, Herrick SR, Ince TA, Kleinman MS, Dal Cin P, Morton CC, et al. Uterine leiomyomata with t(10;17) disrupt the histone acetyltransferase MORF. Cancer Res 2004;64:5570–7.
18. Clayton-Smith J, O'Sullivan J, Daly S, Bhaskar S, Day R, Anderson B, et al. Whole-exome-sequencing identifies mutations in histone acetyltransferase gene KAT6B in individuals with the Say-Barber-Biesecker variant of Ohdo syndrome. Am J Hum Genet 2011;89:675–81.
19. Campeau PM, Kim JC, Lu JT, Schwartzentruber JA, Abdul-Rahman OA, Schlaubitz S, et al. Mutations in KAT6B, encoding a histone acetyltransferase, cause Genitopatellar syndrome. Am J Hum Genet 2012;90:282–9.
20. Simpson MA, Deshpande C, Dafou D, Vissers LE, Woollard WJ, Holder SE, et al. *De novo* mutations of the gene encoding the histone acetyltransferase KAT6B cause Genitopatellar syndrome. Am J Hum Genet 2012;90:290–4.
21. Barretina J, Caponigro G, Stransky N, Venkatesan K, Margolin AA, Kim S, et al. The Cancer Cell Line Encyclopedia enables predictive modelling of anticancer drug sensitivity. Nature 2012;483:603–7.
22. Kahali B, Gramling SJ, Marquez SB, Thompson K, Lu L, Reisman D. Identifying targets for the restoration and reactivation of BRM. Oncogene 2014;33:653–64.
23. Banine F, Bartlett C, Gunawardena R, Muchardt C, Yaniv M, Knudsen ES, et al. SWI/SNF chromatin-remodeling factors induce changes in DNA methylation to promote transcriptional activation. Cancer Res 2005;65:3542–7.
24. Voss AK, Collin C, Dixon MP, Thomas T. Moz and retinoic acid coordinately regulate H3K9 acetylation, Hox gene expression, and segment identity. Dev Cell 2009;17:674–86.
25. Qiu Y, Liu L, Zhao C, Han C, Li F, Zhang J, et al. Combinatorial readout of unmodified H3R2 and acetylated H3K14 by the tandem PHD finger of MOZ reveals a regulatory mechanism for HOXA9 transcription. Genes Dev 2012;26:1376–91.
26. Dreveny I, Deeves SE, Fulton J, Yue B, Messmer M, Bhattacharya A, et al. The double PHD finger domain of MOZ/MYST3 induces α-helical structure of the histone H3 tail to facilitate acetylation and methylation sampling and modification. Nucl Acids Res 2014;42:822–35.
27. Borrow J, Stanton VP Jr, Andresen JM, Becher R, Behm FG, Chaganti RS, et al. The translocation t(8;16)(p11;p13) of acute myeloid leukaemia fuses a putative acetyltransferase to the CREB-binding protein. Nat Genet 1996;14:33–41.
28. Kitabayashi I, Aikawa Y, Yokoyama A, Hosoda F, Nagai M, Kakazu N, et al. Fusion of MOZ and p300 histone acetyltransferases in acute monocytic leukemia with a t(8;22)(p11;q13) chromosome translocation. Leukemia 2001;15:89–94.
29. Doyon Y, Cayrou C, Ullah M, Landry AJ, Côté V, Selleck W, et al. ING tumor suppressor proteins are critical regulators of chromatin acetylation required for genome expression and perpetuation. Mol Cell 2006;21:51–64.
30. Ali M, Yan K, Lalonde ME, Degerny C, Rothbart SB, Strahl BD, et al. Tandem PHD fingers of MORF/MOZ acetyltransferases display selectivity for acetylated histone H3 and are required for the association with chromatin. J Mol Biol 2012;424:328–38.
31. Szakszon K, Berényi E, Jakab A, Bessenyei B, Balogh E, Köbling T, et al. Blepharophimosis mental retardation syndrome Say-Barber/Biesecker/Young-Simpson type—new findings with neuroimaging. Am J Med Genet A 2011;155A:634–7.
32. Szakszon K, Salpietro C, Kakar N, Knegt AC, Oláh É, Dallapiccola B, et al. *De novo* mutations of the gene encoding the histone acetyltransferase KAT6B in two patients with Say-Barber/Biesecker/Young-Simpson syndrome. Am J Med Genet A 2013;161A:884–8.
33. Taipale M, Rea S, Richter K, Vilar A, Lichter P, Imhof A, et al. hMOF histone acetyltransferase is required for histone H4 lysine 16 acetylation in mammalian cells. Mol Cell Biol 2005;25:6798–810.
34. Smith ER, Cayrou C, Huang R, Lane WS, Côté J, Lucchesi JC, et al. A human protein complex homologous to the Drosophila MSL complex is responsible for the majority of histone H4 acetylation at lysine 16. Mol Cell Biol 2005;25:9175–88.

35. Yuan H, Rossetto D, Mellert H, Dang W, Srinivasan M, Johnson J, et al. MYST protein acetyltransferase activity requires active site lysine autoacetylation. EMBO J 2012;31:58–70.
36. Iwakawa R, Takenaka M, Kohno T, Shimada Y, Totoki Y, Shibata T, et al. Genome-wide identification of genes with amplification and/or fusion in small cell lung cancer. Genes Chromosomes Cancer 2013;52:802–16.
37. Daigle SR, Olhava EJ, Therkelsen CA, Majer CR, Sneeringer CJ, Song J, et al. Selective killing of mixed lineage leukemia cells by a potent small-molecule DOT1L inhibitor. Cancer Cell 2011;20:53–65.
38. Zuber J, Shi J, Wang E, Rappaport AR, Herrmann H, Sison EA, et al. RNAi screen identifies Brd4 as a therapeutic target in acute myeloid leukaemia. Nature 2011;478:524–8.
39. Delmore JE, Issa GC, Lemieux ME, Rahl PB, Shi J, Jacobs HM, et al. BET bromodomain inhibition as a therapeutic strategy to target c-Myc. Cell 2011;146:904–17.
40. Dawson MA, Prinjha RK, Dittmann A, Giotopoulos G, Bantscheff M, Chan WI, et al. Inhibition of BET recruitment to chromatin as an effective treatment for MLL-fusion leukaemia. Nature 2011;478:529–33.
41. Vonlaufen N, Naguleswaran A, Coppens I, Sullivan WJ Jr. MYST family lysine acetyltransferase facilitates ataxia telangiectasia mutated (ATM) kinase-mediated DNA damage response in Toxoplasma gondii. J Biol Chem 2010;285:11154–61.
42. Jett JR, Schild SE, Kesler KA, Kalemkerian GP. Treatment of small cell lung cancer: Diagnosis and management of lung cancer, 3rd ed: American College of Chest Physicians evidence-based clinical practice guidelines. Chest 2013;143:e400S–19S.
43. Kebede AF, Schneider R, Daujat S. Novel types and sites of histone modifications emerge as players in the transcriptional regulation contest. FEBS J 2015;282:1658–74.
44. Rothbart SB, Strahl BD. Interpreting the language of histone and DNA modifications. Biochim Biophys Acta 2014;1839:627–43.
45. Schiltz RL, Mizzen CA, Vassilev A, Cook RG, Allis CD, Nakatani Y, et al. Overlapping but distinct patterns of histone acetylation by the human coactivators p300 and PCAF within nucleosomal substrates. J Biol Chem 1999;274:1189–92.
46. Hashizume R, Andor N, Ihara Y, Lerner R, Gan H, Chen X, et al. Pharmacologic inhibition of histone demethylation as a therapy for pediatric brainstem glioma. Nat Med 2014;20:1394–6.
47. Papazyan R, Voronina E, Chapman JR, Luperchio TR, Gilbert TM, Meier E, et al. Methylation of histone H3K23 blocks DNA damage in pericentric heterochromatin during meiosis. Elife 2014;3:e02996.

Published OnlineFirst July 24, 2015; DOI: 10.1158/0008-5472.CAN-14-3702

Cancer Research
The Journal of Cancer Research (1916–1930) | The American Journal of Cancer (1931–1940)

AACR American Association for Cancer Research

KAT6B Is a Tumor Suppressor Histone H3 Lysine 23 Acetyltransferase Undergoing Genomic Loss in Small Cell Lung Cancer

Laia Simó-Riudalbas, Montserrat Pérez-Salvia, Fernando Setien, et al.

Cancer Res 2015;75:3936-3945. Published OnlineFirst July 24, 2015.